

# Ion-velocity-dependent track formation in yttrium iron garnet: A thermal-spike analysis

G. Szenes

*Institute for General Physics, Eötvös University, Muzeum krt 6-8, H-1088 Budapest, Hungary*

(Received 12 July 1994; revised manuscript received 16 March 1995)

Experimental data on track formation in yttrium iron garnet (YIG) are analyzed using a thermal-spike model. Good agreement between predictions and the data is found. For irradiations with low and high ion velocities the efficiency of the energy deposition in the thermal spike is 35 and 19%, respectively, leading to a lower damage cross section  $A$  in the latter case. When  $A$  is plotted versus the energy deposited in the thermal spike, all track data follow a single curve. The variation of  $A$  due to the broadening of the  $\delta$ -electron energy distribution with ion velocity is discussed.

## I. INTRODUCTION

In the last few years a systematic investigation of latent track formation was reported in yttrium iron garnet (YIG).<sup>1-3</sup> Numerous experimental data and extensive studies were published on YIG irradiated with different ions in the electronic stopping regime. The characteristic features of the irradiation effects have been recognized in the experiments, and it was shown that latent tracks are mostly cylinders with amorphous structure. At equal electronic stopping powers  $S_e$ , a variation of the track size with ion velocity was also reported,<sup>3</sup> as shown in Fig. 1. Since it is reasonable to suppose that this velocity effect is not restricted to YIG only, it is of general importance to study this effect in more detail.

The aim of the present paper is to contribute to the understanding of the phenomenon by applying the thermal-spike model proposed in Refs. 4 and 5 and also to formulate the consequences of the physical picture proposed in Ref. 3 in a form suitable to be quantitatively checked in experiments.

## II. APPLICATION OF THE THERMAL-SPIKE MODEL

A thermal spike is a high-temperature region formed along the trajectory of an energetic ion. If  $S_e$  is

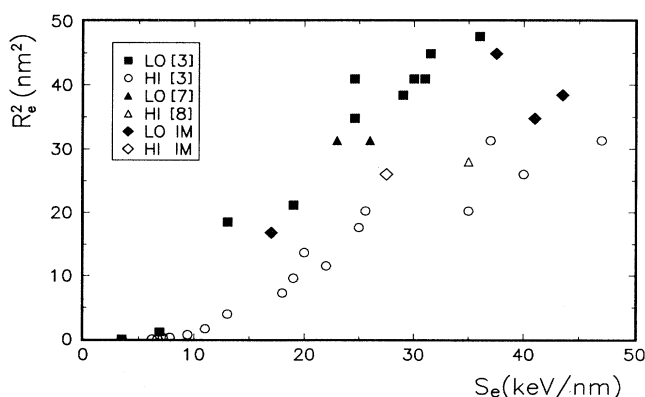


FIG. 1. Experimental data obtained with low-velocity (LO) and high-velocity (HI) ion irradiations. The IM data belong to the 2.2 MeV/nucleon  $< E < 7.6$  MeV/nucleon range (Ref. 3);  $R_e$ : experimental latent track radius.

sufficiently high, then the material (crystalline or amorphous) is melted within a cylinder. The high cooling rate may result in the formation of an amorphous phase. The model is based on two assumptions: (i) the radial distribution of the temperature increase is approximated by a Gaussian function in the phonon system with an initial width  $a(0)$  and (ii) the radius of the melted ( $R_0$ ) and the experimentally determined amorphized cylindrical volumes ( $R_e$ ) are equal. In the approximation applied in Ref. 5 the model provides the following equations for  $R_0$ :

$$R_0^2 = a^2(0) \ln[(gS_e)/(\rho\pi c a^2(0)T_0)] , \quad 2.7S_{et} \geq S_e \geq S_{et} , \quad (1)$$

$$R_0^2 = gS_e/2.7c\rho\pi T_0, \quad S_e \geq 2.7S_{et} , \quad (2)$$

$$S_{et} = \rho\pi c a^2(0)T_0/g , \quad (3)$$

where  $gS_e$  is the fraction of  $S_e$  deposited in the thermal spike, and  $c$ ,  $\rho$ , and  $T_0$  are the mean specific heat, the density, and the difference between the melting and target temperatures, respectively.

We have already analyzed the experiments on latent track formation in different magnetic insulators irradiated with high-velocity ion beams.<sup>5</sup> We took  $a(0) = \text{const}$  in the analysis and this worked well for high-velocity ion-beam experiments. However, a different approach<sup>3</sup> leads to the assumption that  $a(0)$  may vary with the velocity of the ions. Below, we shall discuss how this assumption can be incorporated in our model and what are the expected consequences.

Meftah *et al.*<sup>3</sup> characterized the energy distribution in the electron system by the so-called Waligorski radius  $R_d$ , which is the radius of a cylinder in which 66% of the  $S_e$  is deposited. The values of  $R_d$  depend on the ion velocities and they were calculated in Ref. 3 according to the analytical expression given in Ref. 6 for the radial energy distribution of  $\delta$  electrons. Meftah *et al.* showed that by introducing  $R_d$  for the characterization of the spatial energy distribution, the differences between the damage cross sections in low-velocity (LO) and high-velocity (HI) irradiation experiments could be qualitatively understood.

In our model  $a(0)$  has a similar meaning in the phonon system as  $R_d$  has in the electron system. In the case of a Gaussian temperature distribution, 63% of the thermal

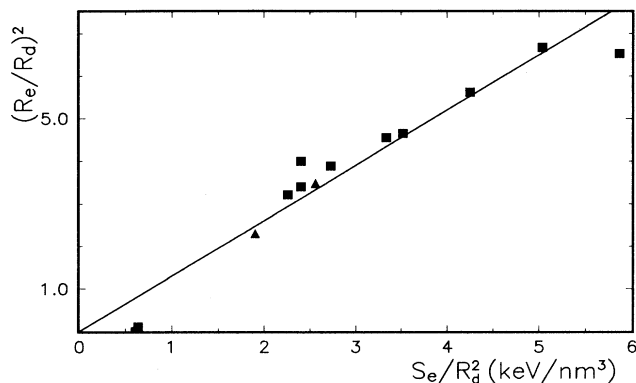


FIG. 2. Normalized plot of the LO data (see Fig. 1 for legend).  $R_e$ : experimental latent track radius; the  $R_d$  values were taken from Ref. 3. The solid line is a least-squares fit omitting the two lowest points.

energy is confined in a cylinder with a radius of  $a(0)$ . Since the source of thermal energy is the energy deposited by the ion in the electron system, it is reasonable to suppose that a correlation exists between  $R_d$  and  $a(0)$ . In the following it will be assumed that this is a simple linear functional relationship,

$$a^2(0) = kR_d^2, \quad (4)$$

with  $k = \text{const.}$

After introducing Eq. (4) into Eqs. (1)–(3), it is a reasonable choice to normalize the variables by  $R_d$  in the appropriate plots. In Figs. 2 and 3  $(R_e/R_d)^2$  versus  $S_e/R_d^2$  is depicted for LO and HI data, respectively. The data for  $R_e$ ,  $R_d$ ,  $E$ , and  $S_e$  were taken from Ref. 3. They were completed with some experimental results.<sup>7,8</sup> Compared to Fig. 1 the IM data belonging to the intermediate range 2.2 MeV/nucleon  $< E < 7.6$  MeV/nucleon were not included in the analysis. It was realized that in this interval the track formation is characteristic neither to LO nor to HI behavior. The size of the IM range was found according to the deviation of experimental points from the general trend towards the HI/LO behavior.

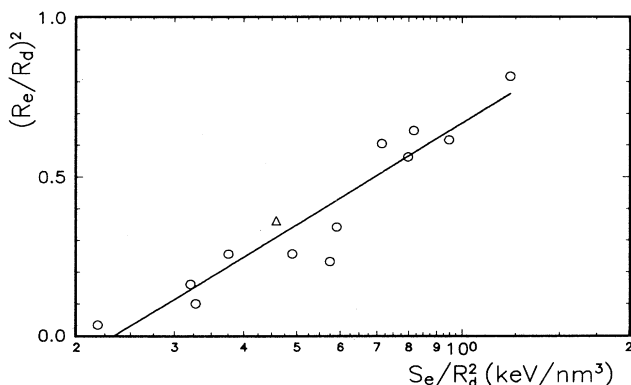


FIG. 3. Normalized plot of the HI data (see Fig. 1 for legend).  $R_e$ : experimental latent track radius; the  $R_d$  values were taken from Ref. 3. The solid line is a least-squares fit.

The LO data in Fig. 2 clearly belong to the linear regime. A straight line starting from the origin can be fitted through them, as required by Eq. (2). The slope of this line does not depend on  $a(0)$  or on the value of  $k$ , only on  $g$  and material parameters. The analysis of the logarithmic dependence was not performed for LO irradiation since we have little experimental data in this range. Thus,  $k_{LO}$  and values of  $a(0)$  were not determined.

The HI points shown in Fig. 3 have much larger scatter, especially at high-energy densities. Nevertheless, a logarithmic dependence can be fitted to most of the points. The shape of the curves in Figs. 2 and 3 agrees with the predictions of the model and the following parameter values were obtained from the analysis based on Eqs. (1)–(3):  $g_{LO} = 0.35$ ,  $g_{HI} = 0.19$ , and  $k_{HI} = 0.46$ . By using the  $k_{HI}$  and  $R_d$  data,  $\langle a(0)^2 \rangle = 21.6 \text{ nm}^2$  was provided by Eq. (4) for the mean value for HI conditions.

### III. DISCUSSION

In Ref. 5 the experimental data on latent track formation obtained in HI irradiation experiments were analyzed for YIG,  $\text{BaFe}_{12}\text{O}_{19}$ ,  $\text{SrFe}_{12}\text{O}_{19}$ ,  $\text{MgFe}_2\text{O}_4$ ,  $\text{NiFe}_2\text{O}_4$ , and  $\text{ZnFe}_2\text{O}_4$ . We showed that latent track formation occurs at  $S_e > S_{et}$ . We also proved that Eq. (1) is fulfilled for  $2.7S_{et} > S_e > S_{et}$  and  $S_{et}$  is related to material parameters through Eq. (3). A remarkable uniform behavior was discovered:  $a(0) = 4.5 \text{ nm}$  and  $g = 0.17$  are valid for all magnetic insulators listed above. These values are in good agreement with the present results though they were obtained in an analysis assuming that  $a(0)$  does not vary with ion velocity. The existence of a linear regime in the track formation was not observed, because it would have required higher  $S_e$  values, which were not available in the HI experiments. In the present study, the analysis of the LO irradiation data clearly indicates (see Fig. 2) that the linear regime exists and it can also be observed in suitable experimental conditions.

It has been shown in Ref. 5 that in the  $R_e^2 - \ln S_e$  plot a straight line can be fitted to the HI data. In Fig. 3 again a straight line is fitted to the HI data, this time in a  $(R_e/R_d)^2 - \ln(S_e/R_d^2)$  plot. This is due to the fact that the  $y \sim \ln x$  function is not very sensitive to such a transformation when the variation is limited to  $5.6 \text{ nm} \leq R_d \leq 8.8 \text{ nm}$ .<sup>3</sup> Moreover, the scatter of experimental points is rather large compared to the expected deviations from linearity. Obviously, the normalization by  $R_d$  has no significance for the linear regime.

It was recognized that the fraction of  $S_e$  deposited in the thermal spike of the phonon system may vary, depending on the target material and the velocity of the ion. In LO irradiations 35% of  $S_e$  is transferred to the thermal spike while in HI experiments only 19%. The reduction of the effectiveness of irradiation with increasing ion velocity has been previously observed in different irradiation experiments, e.g., in track etching,<sup>9</sup> in inelastic sputtering of inorganic and biomolecular compounds,<sup>10</sup> and recently in biological cell inactivation.<sup>11</sup> Revealing the origin of the existing similarities may lead to a better understanding of the phenomenon. However, the comparison of different irradiation effects observed in

different materials is difficult because even the study of the same effect—track formation in mica—by various experimental methods shows qualitatively diverse results.<sup>12</sup>

According to Eq. (2), in a  $R_e^2$ - $gS_e$  plot the line fitted to the data goes through the origin and its slope depends only on material parameters  $c$ ,  $\rho$ , and  $T_0$ , and it is independent of  $a(0)$ . Thus, for a given material in a  $R_e^2$ - $gS_e$  plot the variation of LO and HI data must follow the same line in the linear regime, since the other parameters are identical for both cases. In general, the logarithmic and the linear regimes join at  $S_{e0} = 2.7S_{et}$  where  $R_e = a(0)$ . If  $a(0)$  is velocity dependent then the  $S_{et}$  values are different for the LO and HI data. Therefore, a separation of the LO and HI curves in the logarithmic regime is expected for YIG, and the start of the linear regime (or the end of the logarithmic regime) occurs at different levels of the damage cross sections.

In Fig. 4 the  $R_e^2$  values are plotted versus the energy  $gS_e$  deposited in the thermal spike with  $g = g_{LO}$  and  $g = g_{HI}$  for the LO and HI data, respectively. The solid line is a best fit to the LO data obtained from an analysis with normalization by  $R_d^2$ . The dotted lines show the expected variation in the logarithmic regime (see below). In this figure the tracks with  $g_{HI}S_e > g_{HI}S_{e0} \approx 6$  keV/nm are formed already in the linear regime and they overlap with the LO data in this range. These HI data clearly fit to the LO data in the same  $gS_e$  range. The smooth transition is the indication that experimental LO and HI points follow a common curve in the linear regime.

We estimated  $g_{LO}$  from the slope of the  $(R_e/R_d)^2$ - $S_e/R_d^2$  plot of the LO data in Fig. 2. The value of  $g_{HI}$  was independently obtained from the intersection of the  $(R_e/R_d)^2$ - $\ln(S_e/R_d^2)$  plot of the HI data in Fig. 3. Without scaling the  $R_e^2$  axis, only by using these two independent parameters as weight factors, the linear LO and logarithmic HI curves smoothly fit to each other, as seen in Fig. 4. This behavior is predicted by Eqs. (1) and

(2). This is an important evidence supporting our model and it also confirms that the physical picture and the approximations we use are correct. It also suggests that the efficiency is identical in the linear and the logarithmic regimes for HI conditions.

This overlapping proves that at  $gS_e > 6$  keV/nm "the damage cross-section velocity effect" can be completely accounted for by the difference in the fraction of energies deposited in the thermal spike. Since in the linear regime the damage cross section  $A = \pi R_e^2$  does not depend on  $a(0)$ , it is irrelevant whether  $a(0)$  varies in this range with the ion velocity or not. The variation of a single parameter— $g$ —is sufficient for the phenomenological description. The analysis of the origin of the difference between  $g_{LO}$  and  $g_{HI}$  is beyond the scope of the present paper.

If  $a(0)$  varies with ion velocity, then—in addition to the variation of  $g$ —it may also contribute to the "damage cross-section velocity effect," when  $gS_e < 6$  keV/nm. The separation of the logarithmic part of the LO and HI curves can be used as a check of the variation of  $a(0)$  with ion velocity. The LO and HI curves coincide only if  $a(0)$  is not velocity dependent. In this case, the velocity effect would solely be the consequence of the variation of the  $g$  parameter in the full range of  $S_e$ . The higher the difference in  $a(0)$  is for LO and HI conditions, the larger the separation of the curves in Fig. 4 should be. We evaluated the expected shapes using Eqs. (1) and (2). Since experimental LO data were not sufficient, we assumed that  $k_{LO} = k_{HI}$ . The mean  $a(0)$  values were calculated from Eq. (4) by substituting for  $\langle R_d^2 \rangle$  8.7 nm<sup>2</sup> and 47 nm<sup>2</sup> for LO and HI data, respectively.<sup>3</sup> The dotted curves in Fig. 4 were obtained according to Eq. (1) with mean  $a(0)$  values for the LO and HI cases.

Although the calculations are approximate due to the application of mean values, they correctly characterize the consequences of the variation of  $a(0)$  with the Waligorski radii. In the linear regime the slope is not affected; however, the position of the experimental points along the lines is different in two kinds of plots (plain or normalized). Naturally, the best linear fits are not identical in the two cases, either. It is not possible to reject or confirm the variation of  $a(0)$  with  $R_d$  having experimental data only in this range.

We cannot confirm the variation of  $a(0)$  with  $R_d$  based on the reported LO data in the logarithmic regime, either. However, the significance of the deviation of the existing few data points from the predicted dotted LO curve in Fig. 4 should not be overestimated. Nevertheless, if the actual experimental errors are not significantly larger than those given in Ref. 3, the present set of data suggests that if  $a(0) \neq \text{const}$  then the variation of  $a(0)$  is less sensitive to the ion velocity than the Waligorski radius, i.e.,  $k_{HI} < k_{LO}$ . More data are necessary to clear up this point.

Our analysis offers a simple explanation of the variation of the damage efficiency  $\epsilon$  with  $S_e$  reported in Ref. 3. In HI experiments most of the latent tracks are formed in the logarithmic regime and a few in the linear regime. In the logarithmic regime  $\epsilon = A/S_e \sim \ln(S_e/S_{et})/S_e$  in-

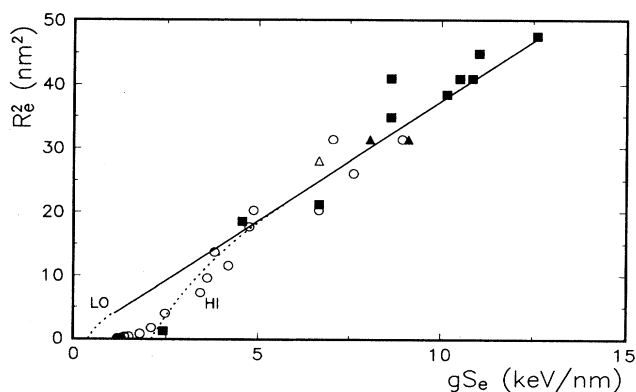


FIG. 4. Experimental data plotted versus the energy deposited in the thermal spike  $gS_e$  (see Fig. 1 for legend). The dotted curves are calculated according to Eq. (1) with different mean  $a(0)$  values for LO and HI irradiations (see text). The solid line is a least-squares fit to LO data omitting the two lowest points.

creases with  $S_e$  up to  $S_e \approx 2.7S_{et} = 31$  keV/nm and in the linear regime obviously  $\epsilon = \text{const}$ . This is the origin of the saturation behavior observed by Meftah *et al.*<sup>3</sup>

In LO experiments a maximum of  $\epsilon$  was reported.<sup>3</sup> Our analysis indicates that LO tracks are formed in the linear regime leading to  $\epsilon = \text{const}$ . Our opinion is that the decrease of  $\epsilon$  is due to tracks obtained in experiments with ions in the intermediate velocity range (see IM points in Fig. 1). In this range a transition between the LO and HI behavior is expected. In IM experiments the efficiency of energy deposition is lower than for LO and higher than for HI irradiations. The mixing of the LO and IM data in the analysis caused the apparent maximum in the variation of  $\epsilon$  versus  $S_e$ . When IM points are omitted,  $\epsilon = \text{const}$  within the experimental errors. Thus, our analysis provides a clear explanation of the variation of damage efficiency in YIG.

According to the analysis of HI data, the transition between the linear and logarithmic regimes occurs at about  $gS_e = 6$  keV/nm. At the transition point, the peak temperature of the thermal spike  $T_p = 2.7T_0 \approx 4100$  K. Note that  $T_p$  can be obtained from the present analysis only for HI conditions, because we do not know  $a(0)$  for LO irradiations. If we accept as an estimate that  $k_{LO} = k_{HI}$ , then the transition occurs for LO conditions at about  $gS_e = 1.1$  keV/nm and  $T_p \approx 22100$  K at  $g_{LO}S_e = 6$  keV/nm. Probably  $k_{HI} < k_{LO}$ , however, therefore  $22100 \text{ K} > T_p \geq 4100$  K is expected. Since most of the LO data were measured

above  $gS_e = 6$  keV/nm and most of the HI data below it, we conclude that HI tracks were formed in thermal spikes typically with  $T_p \leq 4100$  K and LO tracks with  $T_p \geq 4100$  K.

## VI. CONCLUSIONS

A model of a thermal spike formed in high-energy heavy-ion irradiation experiments was applied to track formation in YIG and good agreement with mean experimental data was found. The analysis shows that while for LO irradiation 35% of  $S_e$  is deposited in the thermal spike, this figure is only 19% for HI irradiation. This difference is responsible for the "damage cross-section velocity effect" for  $gS_e > 6$  keV/nm. A second contribution is also possible for  $gS_e < 6$  keV/nm if  $a(0)$  varies with ion velocity. It is proposed that the study of the separation of the  $R_e^2 gS_e$  curves for LO and HI irradiations provides a suitable check of the existence of this contribution.

## ACKNOWLEDGMENT

The author is grateful to Dr. M. Toulemonde for turning his attention to this problem and also for stimulating discussions. This work was carried out in CIRIL (France) during the stay of the author supported by the Commission of the European Communities as part of the European Economic Community mobility action.

<sup>1</sup>P. Hansen, H. Heitmann, and P. H. Smit, Phys. Rev. B **26**, 3539 (1982).

<sup>2</sup>F. Studer *et al.*, Radiat. Eff. Def. Solids **116**, 59 (1991).

<sup>3</sup>A. Meftah *et al.*, Phys. Rev. B **48**, 920 (1993).

<sup>4</sup>G. Szenes, Mater. Sci. Forum **97-99**, 647 (1992).

<sup>5</sup>G. Szenes, Phys. Rev. B **51**, 8026 (1995).

<sup>6</sup>M. P. R. Waligorski, R. N. Hamm, and R. Katz, Nucl. Tracks Radiat. Meas. **11**, 309 (1986).

<sup>7</sup>A. Meftah (private communication).

<sup>8</sup>J. M. Constantini *et al.*, Nucl. Instrum. Methods Phys. Res., Sect. B **91**, 288 (1994).

<sup>9</sup>R. L. Fleischer, P. B. Price, R. M. Walker, and E. L. Hubbard, Phys. Rev. **156**, 353 (1967).

<sup>10</sup>I. A. Baranov, Yu. V. Martynenko, S. O. Tsepelevich, and Yu. N. Yavlinskii, Usp. Fiz. Nauk **156**, 477 (1988) [Sov. Phys. Usp. **31**, 1015 (1988)].

<sup>11</sup>A. Chetoui *et al.*, Int. J. Radiat. Biol. **65**, 511 (1994).

<sup>12</sup>G. Szenes (unpublished).